The formation, character and changing nature of mesoscale convective systems

Russ S. Schumacher ✉ *and Kristen L. Rasmussen*

Abstract | Mesoscale convective systems (MCSs) describe organized groupings of thunderstorms in the tropics and mid-latitudes that span thousands of square kilometres. While recognized for over a century, the advent of satellite and radar observations, as well as atmospheric-model simulations, has brought about their increased understanding. In this Review, we synthesize current knowledge on MCS formation, climatological characteristics, hazardous weather, predictive capacity and projected changes with anthropogenic warming. Driven by typical deep moist convective processes (moisture, lift and instability) and vertical wind shear, MCS formation occurs preferentially in locations where these ingredients are present and can be maintained by large-scale ascent and the cold pools that they produce. MCSs also generate hazardous weather, including extreme rainfall, flooding, derechos and, sometimes, tornadoes and hail, all of which have substantial economic and societal impacts. Given that MCSs also produce a large fraction of warm-season rainfall, there is critical need for both short-term forecasts and long-term projections, presently challenged by inadequate model resolution. Yet, with continually improving modelling capabilities, as well as greater theoretical basis, it is suggested that MCSs might increase in frequency and intensity under a warming climate. Further modelling progress, in turn, offers improved understanding of MCS characteristics, from their life cycle through to impacts.

Thunderstorms, known more formally as deep moist convection, are a regular meteorological feature across many parts of the world. Their development requires two basic building blocks: an updraft, wherein warm, moist air rapidly rises, forming characteristic cumulonimbus clouds, and a downdraft, which brings rain and evaporatively cooled air back to the surface, creating a cold pool. These individual convective cells, consisting of a single updraft and downdraft, often interact to form storm clusters, lines or complexes. Such groupings are collectively termed mesoscale convective systems (MCSs), encompassing nearly all organized convection that has a length scale of >100 km in one or more directions, and lasting 3 hours or longer.

Following the emergence of radar and satellite-based observations of weather systems, various categories of MCSs have been identified, often centred on their shape (FIG. 1). For example, large, near-circular systems are referred to as mesoscale convective complexes[1] (MCCs; FIG. 1a), whereas those with one long and one narrow axis are referred to as quasilinear convective systems (QLCSs)[2] or squall lines (FIG. 1b), which also include a subset of features such as bow echoes[3] (FIG. 1c). As further study revealed differences in precipitation production and hazards among MCSs, additional classifications were established based on the location of lighter stratiform rain with respect to the convective line, including trailing-stratiform, leading-stratiform and parallel-stratiform structures[4]. Moreover, additional categorizations have been made for those that do meet the typical characteristics of QLCSs, such as the training line/adjoining stratiform (TL-AS; FIG. 1d) and back-building/quasistationary (BB; FIG. 1e) patterns that produce extreme precipitation[5].

MCSs are responsible for a large proportion of tropical through mid-latitude extreme-precipitation events and are, thus, an important component of the hydrologic cycle. Indeed, the rainfall associated with MCSs has aided motivation for expanded research in recent decades. MCSs, for example, bring essential precipitation — and, therefore, water resources — to agriculturally productive regions throughout the tropics and mid-latitudes, such as the Great Plains of the USA, the Sahel and much of Asia. Changes in the frequency of MCSs thus exert a dominant control on rainfall variability in these regions: too few MCSs in a given year facilitates drought conditions, whereas too many promote flooding[6–8]. MCSs are often further associated with hazardous weather; severe winds, flash floods, large hail, lightning and (occasionally) tornadoes can be destructive and deadly[9–11]. For instance, the devastating flood in Pakistan in 2010 (REF.[12]) and the

Department of Atmospheric Science, Colorado State University, Fort Collins, CO, USA.

✉*e-mail: russ.schumacher@colostate.edu*

https://doi.org/10.1038/s43017-020-0057-7

Key points

- Organized lines or clusters of convective storms — known as mesoscale convective systems (MCSs) — frequently occur across the global tropics, subtropics and mid-latitudes.
- MCSs produce over half of the annual rainfall in some regions and provide critical water resources for agriculture in those regions.
- Much of the extreme rainfall in mid-latitude land areas comes from MCSs, often causing deadly and destructive flash flooding. MCSs are also responsible for widespread damaging wind events, called derechos.
- MCS organization, structure and maintenance is governed by the ingredients for deep moist convection (moisture, instability and lift) and by how vertical wind shear interacts with convective updrafts and cold pools.
- Prediction of MCS rainfall and hazards is a major challenge, owing to multiscale processes and insufficient resolution of atmospheric models. Yet, predictions are improving with advances in understanding and computing.
- Understanding how MCSs will change in a warmer climate is a new and important research area. Results thus far suggest that heavy rainfall from MCSs is likely to increase.

derecho in the eastern USA in 2012 (REF.[13]) caused major societal disruption.

Given the hydrologic importance and hazardous nature of MCSs, there is a key need to understand their characteristics, especially against a background of climatic warming that is anticipated to influence their properties. For instance, evidence suggests that the environmental conditions favouring MCS formation may increase[14,15], so too may MCS rainfall rates and volumes[16–18]. Thus, while MCSs have long been recognized and studied[19,20], a wealth of new literature has emerged with the objective of enhancing understanding of their fundamental characteristics, in turn, improving forecasts, hazard warnings, water-resource management and climate projections.

In this Review, we synthesize the latest understanding of MCSs, beginning with their climatological characteristics and formation mechanisms. The hazards and impacts associated with MCSs are subsequently discussed, followed by the current state of predictability and responses to anthropogenic warming. The Review ends by outlining priority questions that remain for future research.

The climatology of MCSs

Considering the temporal and spatial scales associated with MCSs (>100 km and >3 h), comprehensive documentation of where and when they occur was not possible until radar and infrared satellites were broadly deployed. Infrared brightness temperature data from geostationary satellites, for example, first became available in the 1970s, resulting in the identification and widely used definition of MCCs[1]. The polar-orbiting Tropical Rainfall Measuring Mission (TRMM) satellite, which operated from 1998 to 2015, further enabled unprecedented observations of MCSs in the tropics and subtropics[6,21]. Owing to their lack of temporal continuity, however, such polar-orbiting satellites only provide opportunities for MCSs to be sampled in snapshots[22].

Ground-based radar networks, by contrast, provide opportunity for detailed examination of MCS characteristics, albeit constrained to land areas and those nations with sufficient resources to deploy them, such as Europe[23], the USA, India[24], China[25], Taiwan[26] and South Korea[27]. While radar-based analyses have historically involved manual examination of large quantities of radar animations[4,5,28,29], new algorithms have recently allowed for comprehensive, automated identification and tracking of MCSs[7,30–32], advancing understanding of their climatological characteristics. Here, we begin by outlining the typical spatial and temporal features of MCSs garnered from the remote-sensing observations.

Spatial climatologies. Analyses of satellite and ground-based radar observations have provided exceptional insight into the spatial characteristics of MCSs, revealing thousands of occurrences per year globally, of which ~400 of the largest develop in favoured locations focused in the tropics, subtropics and mid-latitudes[6,33].

MCSs, for example, are common throughout land regions of tropical and subtropical South America, Africa, South Asia and the Maritime Continent[6,33,34]. As a result, TRMM observations show that, tropics-wide, MCSs are the dominant source of rainfall, contributing over half (typically 50–90%) of annual precipitation totals[6,35–37] (FIG. 2), and demonstrating their critical importance in local hydrological cycles. In the La Plata Basin of South America, for instance, >90% of summertime precipitation is from MCSs[36], whereas in the Sahel and Congo Basin, contributions exceed 70%[6,38]. It must be noted, however, that the inability of polar-orbiting satellites to observe the temporal continuity of MCSs introduces some uncertainty to these quantitative estimates, overestimating the fraction of deep convective storms that last long enough to be MCSs[22]. Nevertheless, in the tropics, MCS occurrence has been linked to the Mei-Yu front in tropical East Asia[26], Bay of Bengal depressions and the southeast Asian monsoon[39], orographic-induced gravity waves off the coast of Colombia in the tropical West Pacific[40], tropical easterly waves over the Sahel region of Africa[38], coastal squall lines in north-eastern South America[41] and the Madden–Julian Oscillation in the central Indian Ocean through Maritime Continent regions[42].

MCSs are also commonly observed in the mid-latitudes, particularly in central North America[7] (FIG. 3). Indeed, in the USA, MCSs are very frequent in the central and eastern states, wherein 500–700 are counted each year[7] (FIG. 3a). Here, substantial seasonal variability is also apparent, with most occurring in the central states (for example, Kansas and Missouri) during May–August (FIG. 3b), moving to the eastern states (for example, Tennessee, Mississippi, Alabama and Georgia) during September–April[7,43] (FIG. 3c). Similar to the tropics, radar observations in the USA further indicate that MCSs contribute a significant proportion of precipitation, totalling ~40% of annual (FIG. 3d) and >60% of warm-season (May–August; FIG. 3e) rainfall in the Great Plains[7,43].

MCS characteristics differ between the tropical oceans and subtropical or mid-latitude land areas. In the latter, MCSs tend to be more intense, with precipitation coming from a smaller number of large, strong MCSs[35,44]. Some of these differences can be explained

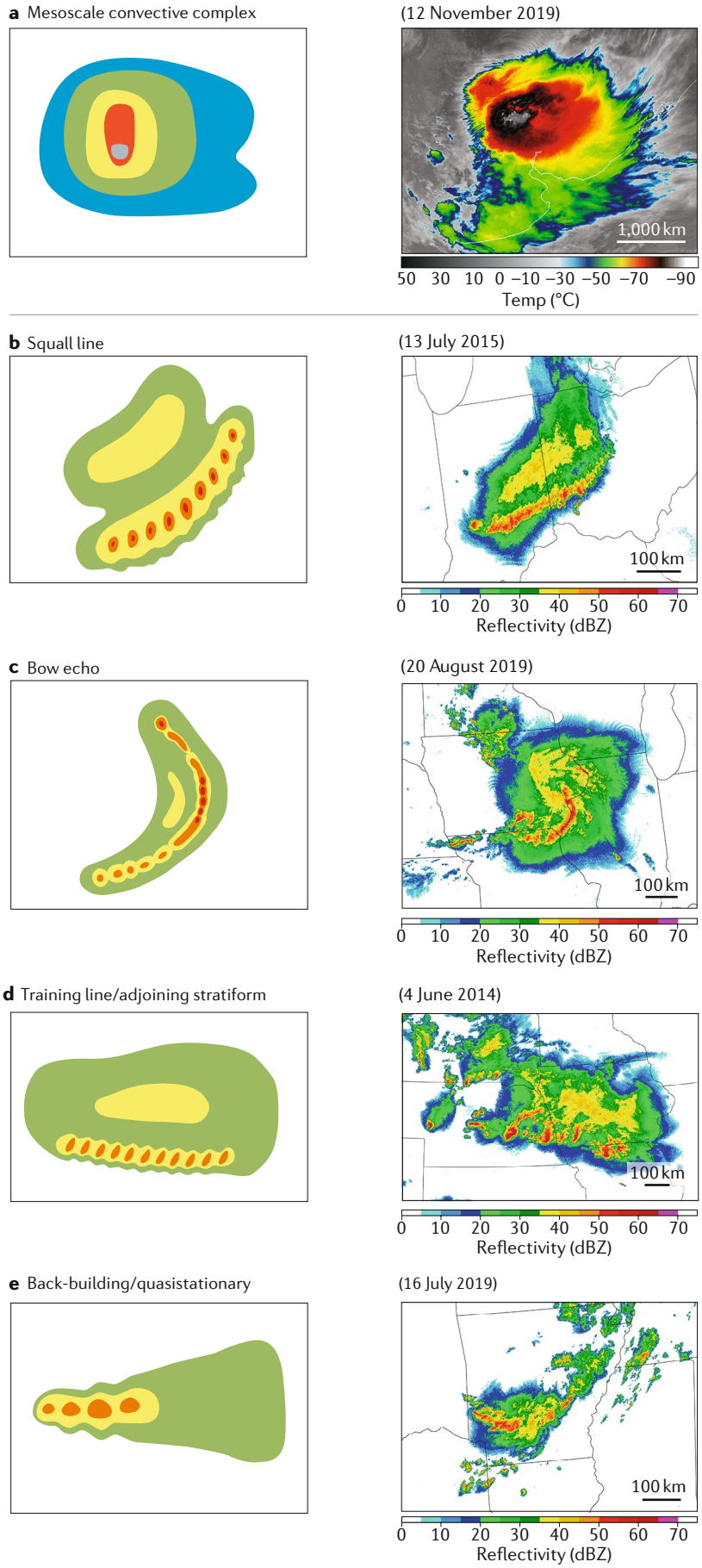

Fig. 1 | **Key MCS types.** Schematic illustration (left) and observed infrared or radar retrievals (right) of a mesoscale convective complex (panel **a**), squall line (panel **b**), bow echo (panel **c**), training line/adjoining stratiform mesoscale convective system (MCS; panel **d**) and back-building MCS (panel **e**). Radar data in panels **b**–**e** are from the Multi-Radar Multi-Sensor system[183]. MCSs can take on a wide variety of structures, with the examples shown here among the most highly organized. Schematics in panels **d** and **e** adapted with permission from REF.[5], © American Meteorological Society.

by the greater vertical wind shear at higher latitudes (owing to the proximity to the subtropical and polar jet streams), which promotes greater MCS organization, as discussed further later.

Temporal variability. In addition to the marked spatial variability, MCSs also exhibit pronounced temporal variability, as alluded to previously when outlining the seasonality in US-based counts and resulting precipitation. Indeed, across the mid-latitudes, a strong seasonal cycle is apparent, with most MCSs occurring predominantly during the warm season, when moisture and instability are most abundant[35]. In continental Europe, for example, the number of MCSs reaches a maximum during May to August (the warm season)[45] and decreases from September, broadly consistent with observations from the central USA[7] and East Asia[46]. In the southern hemisphere, summertime peaks in MCS counts are similarly observed in both the Amazon Basin[47] and the subtropics[36]. At lower latitudes or over the oceans, by contrast, the seasonal cycle is less pronounced[33,35,44]. For example, over Africa, MCS occurrence shifts from north to south of the equator with the seasons, but the frequency remains relatively constant throughout the year[44].

MCSs also exhibit variability at shorter timescales, specifically in regards to a distinct diurnal cycle. Over land, MCSs typically initiate in the afternoon or early evening, owing to increased instability from daytime heating of the land surface, reach maximum intensity overnight and dissipate within a few hours after sunrise[7,33,48–50]. This tendency for MCSs to be strongest overnight is associated with low-level jets — confined areas of strong winds that are a common feature of continental regions to the east of mountain ranges[51] — that develop after dark, transport warm, moist air polewards and cause air to ascend, which fuels MCS intensification[52]. The diurnal cycle can vary geographically: a strong nocturnal maximum is apparent in the Great Plains of the USA, but in the south-eastern USA, there is a greater frequency of occurrence in the afternoon and evening[7]. Over the oceans, however, because the underlying surface does not respond as sharply to diurnal variations in solar radiation, the diurnal cycle of MCSs is less pronounced[50] (FIG. 2b,c).

Formation, organization and maintenance

Having established the 'where and when', we now discuss the formation and evolution of MCSs, synthesizing information from the larger environmental-scale conditions through to storm-scale processes. A comprehensive examination can also be found in REFS[19,20,53–56].

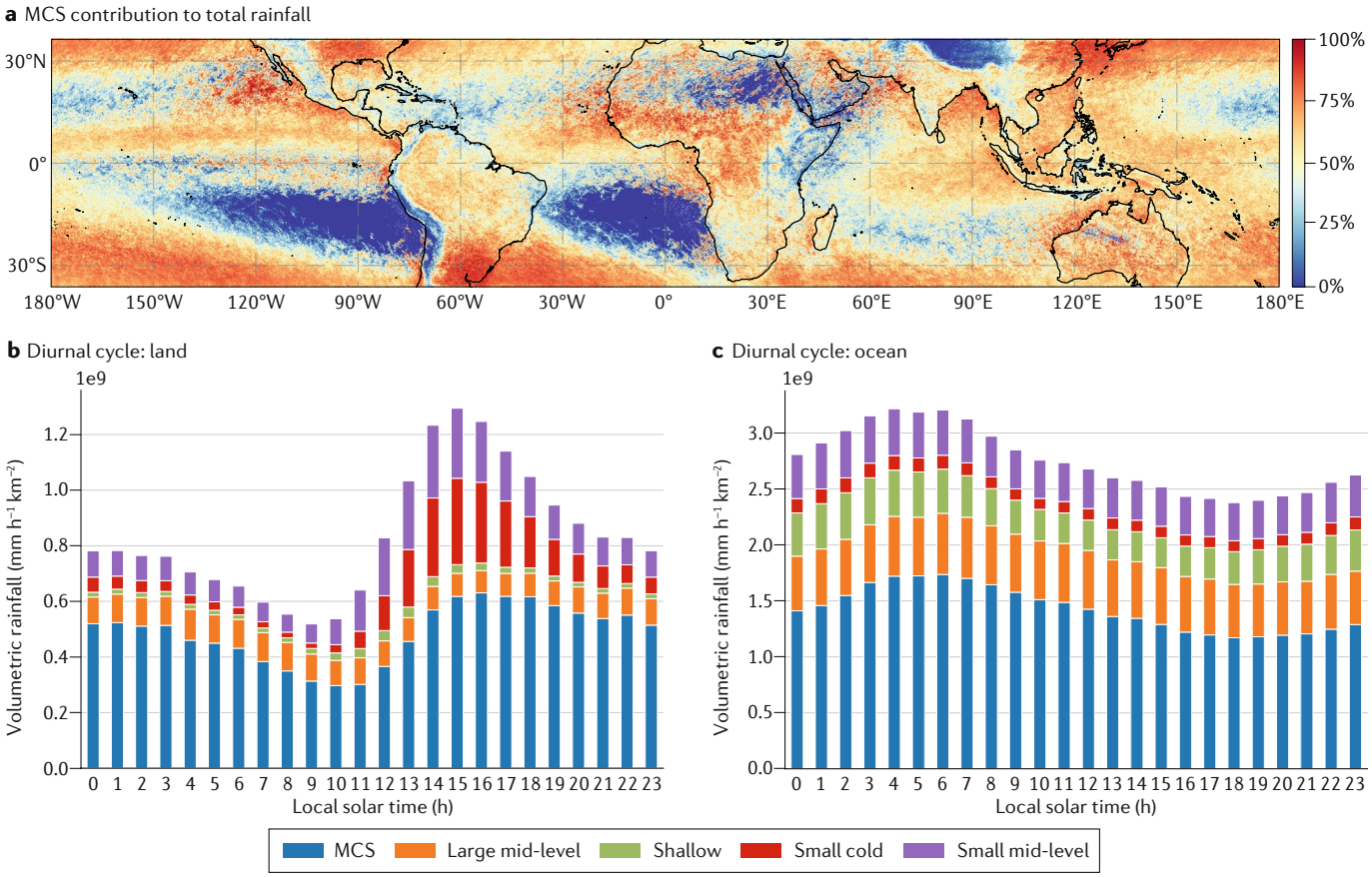

Fig. 2 | **The contribution of MCSs to global rainfall.** Fraction of annual rainfall produced by mesoscale convective systems (MCSs) based on observations from the Tropical Rainfall Measuring Mission (TRMM) satellite between December 1997 and September 2014 (panel **a**). Diurnal cycle of TRMM volumetric rainfall over the land (panel **b**) and ocean (panel **c**) between 36°N/S. In many parts of the global tropics, subtropics and mid-latitudes, MCSs produce a large fraction of the annual precipitation. MCSs over land have a strong diurnal cycle, with rain maximized in the afternoon and evening, and minimized in the morning; MCSs over ocean have a less pronounced diurnal cycle. Panel **a** adapted with permission from REF.[6], © American Meteorological Society. Panels **b** and **c** adapted with permission from REF.[50], © American Meteorological Society.

Fundamental ingredients. An ingredients-based methodology[57] dictates that the following characteristics must be present for deep moist convection to occur: moisture — sufficient atmospheric water vapour to condense to form clouds and precipitation; lift — a mechanism by which air is forced to ascend, such as a front or sloped terrain; and instability — an atmospheric temperature profile in which ascending air parcels become less dense (warmer) than the surrounding air, supporting continued upwards acceleration of those parcels[53]. Collectively, these ingredients can be expressed in regards to convective available potential energy (CAPE), that is, an estimate of the vertically integrated buoyancy of adiabatically lifted air, embracing requirements for moisture and instability[58]. Without these ingredients in place, convective storms will not develop.

For convective storms to organize into larger structures such as MCSs, an additional ingredient is required: vertical wind shear. Describing the change in wind speed and/or direction with height, vertical wind shear alters the way in which cold, downdraft air spreads away from the storm. In the absence of shear, for example, the cold air moves out in a circular pattern over a thin layer upon reaching the ground. However, when shear is present, there is flow towards the cold pool on the downshear side, which slows the spread of the cold pool there. This flow increases the depth of the cold pool, enhancing lift at the edge of the cold pool that may initiate new convective updrafts[53]. As the new cells form their own downdrafts, they merge with the existing cold pool, continuing the process and organizing convection into lines or clusters[53]. Vertical wind shear further influences where new convection develops, in turn, dictating the organization of the MCS[4,59–62]. For example, shear dictates the transport of precipitation particles after formation in the updrafts, affecting both the growth of the cold pool and the latent heat release that occurs at mid-levels. These processes subsequently influence where new updrafts form and, thereby, the development of circulations within the MCS itself. MCSs can form at any orientation with respect to the vertical shear, but assuming a cold pool develops, these processes tend to result in MCSs oriented perpendicular to the shear, where ascent is maximized[4,63].

Differences in the geographic variability of vertical wind shear also help explain the distinctions between

MCSs in the tropics and mid-latitudes. Indeed, shear tends to be relatively weak in the tropics (less than 10 m s^{-1} of difference between the surface and 6 km above ground), producing MCSs with highly varied structures with respect to shear magnitude and direction. In small low-level and mid-level shear tropical environments, convection is arranged in circular, ring-like patterns due to the lack of an organizing mechanism. However, when either low-level or mid-level shear or both are strong, linear MCSs result and are organized either parallel or perpendicular to the shear, depending on the scenario[64,65]. In the mid-latitudes, by contrast, vertical shear tends to be quite strong, promoting highly organized MCSs such as MCCs and bow echoes[66], demonstrating the geographic variability in MCS archetypes.

Given the tendency for MCSs to form preferentially in specific parts of the world, it can be assumed that their large-scale environments are favourable regions for all 'ingredients' to occur together (moisture, lift, instability and shear)[67]. Favoured regions for MCSs, for example, include East Asia, subtropical South America and Africa, and central North America, all of which are downstream of elevated terrain and proximate to a moisture source, such as warm sea surface. Elevated terrain can serve as a lifting mechanism for initial thunderstorms to grow into MCSs, but also fosters the development of low-level jets downstream and allows for clusters of intense storms to initiate through elevated mixed layers[68–70].

Meteorological regimes. With essential ingredients needed for development, MCSs often form in common synoptic environments. For example, in the USA, a large proportion of warm-season MCS activity is associated with two distinct large-scale synoptic patterns: a translating cold front (FIG. 4a) and a quasistationary east–west front[71] (FIG. 4b). Similar synoptic situations, with some regional variations, are also found in MCS environments globally[67].

For a translating cold front (FIG. 4a), forcing for ascent is provided ahead of a mid-tropospheric trough and corresponding surface front. The presence of moist, unstable air ahead of the cold front provides fuel for the generation of fast-moving linear MCSs such as squall lines[32,71,72]. Slower-moving MCSs may also form on the cool side of the trailing stationary front, owing to the lifting of warm, moist air parallel to the upper-level winds[73]. This situation can occur throughout the year, but is especially common in the transition seasons of spring and autumn, when extratropical cyclones and associated frontal systems are frequent[74,75].

MCS formation is also common in a quasistationary east–west front pattern (FIG. 4b), characteristic of the warm season when moist, unstable air is abundant, and relatively weak mid-tropospheric winds and a stationary front or slow-moving warm front are featured at the surface[74,75]. In this pattern, the forcing for ascent may be a subtle shortwave trough in the mid-troposphere or the ascent of air within and ahead of a low-level jet stream that is oriented perpendicular to the surface frontal zone. In particular, when a low-level jet intersects a frontal zone, there is strong low-level warm advection and frontogenesis that promotes the initiation and organization of convection[74,76–79]. MCSs in this environment generally form parallel to the mid-tropospheric winds, but may reorient to become perpendicular to the winds, depending on the wind shear and whether a strong

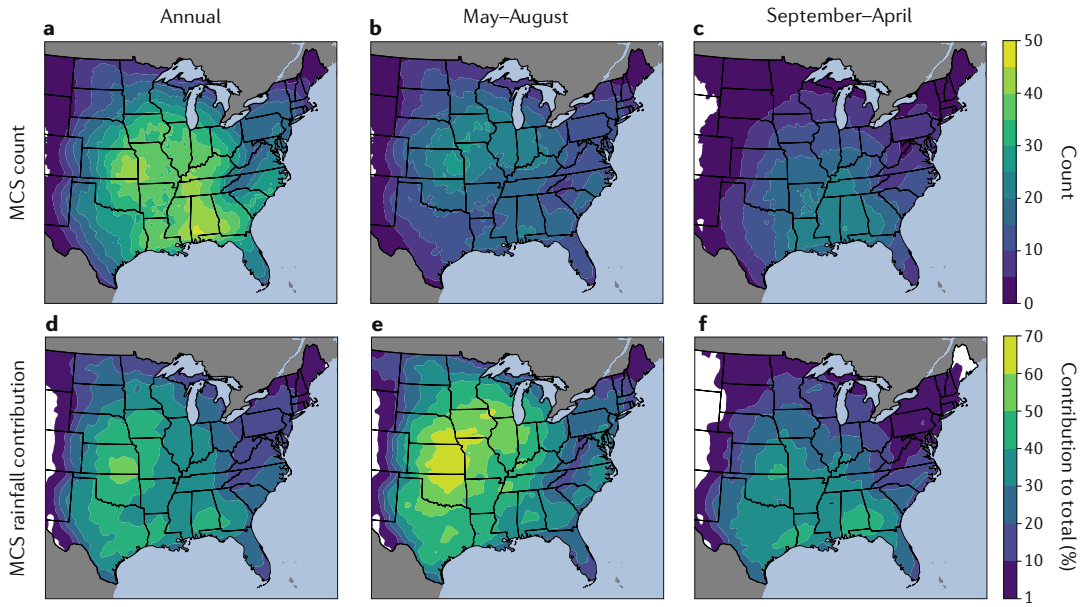

Fig. 3 | **MCS frequency and the rainfall contribution of MCSs in the USA.** Mean mesoscale convective system (MCS) occurrence over the USA for January–December (panel **a**), May–August (panel **b**) and September–April (panel **c**). Percentage contribution of MCS rainfall to total rainfall for January–December (panel **d**), May–August (panel **e**) and September–April (panel **f**). Over the USA, where there is a long record of radar and precipitation data, MCSs are found to be frequent and to contribute over half of the annual rainfall in the agriculturally productive central USA. Adapted with permission from REF.[7], © American Meteorological Society.

cold pool develops[80,81]. Although the details vary geographically, similar environments have been identified in MCS-active regions in Asia and South America[67,68]. Furthermore, these environments can remain in place for a week or more during the warm season, leading to 'corridors' of heavy precipitation within a narrow latitude band[52,82,83].

These meteorological regimes are responsible for setting the stage for organized convective systems, with the dynamics responsible for their organization, maintenance and evolution being a function of both the larger-scale setting and storm-generated processes.

Structure, organization and maintenance. Once the ingredients of moisture, instability, lift and wind shear have come together, convection has initiated and organized into an MCS, they must persist for an MCS to be maintained. Two distinct lifting processes may be responsible for their persistence: lifting at the leading edge of a convectively generated cold pool (so-called internally driven MCSs) and lifting associated with larger-scale forcing for ascent, such as along a warm or stationary front (so-called externally driven MCSs)[48]. Whether an MCS is internally or externally driven exerts a key influence on the resulting structure and organization.

For a mature, cold-pool- (internally) driven MCS such as squall lines or bow echoes (FIG. 5), understanding of the strength and vertical structure has largely centred on RKW (Rotunno, Klemp and Weisman) theory[59,84]. Built around idealized 2D and 3D cloud model simulations, RKW theory argues that squall-line structure is governed by the degree of balance or imbalance between the strength of the cold pool and the magnitude of the vertical wind shear over the depth of that cold pool (specifically, the flux of horizontal vorticity produced at the leading edge of the cold pool compared with the flux of horizontal vorticity associated with the vertical wind shear). For example, if the strength of the cold pool is much stronger than the shear, the convective line will tilt upshear over the cold pool and weaken. Conversely, if the strength of the shear is much larger than the cold pool, the convective line will tilt downshear, and intense updrafts will be unsupported. However, if the two effects are in approximate balance, the convective line will be upright, maximizing the strength of the updraft and, presumably, the MCS. Thus, although cold pools are essential for the structure and maintenance of squall lines, if they become too strong, they may lead to the demise of the MCS.

While RKW theory has been upheld in recent idealized studies[84–86], the applicability to observed squall lines has been questioned on the basis of the most intense squall lines not always occurring in the theoretical 'optimal state'[87]. The theory has also been criticized for not considering the possible importance of shear over the depth of the troposphere or sources of vorticity that influence the MCS other than those at the interface of the inflow and the cold pool[60,87,88].

Several other factors also typify the structure of an internally driven MCS. The flow through cold-pool-driven MCSs, for example, is characterized by a broad region of front-to-rear flow behind the convective line, as well as the development of a rear-inflow jet (FIG. 5). These flow patterns are associated with an expansive region of lighter 'stratiform' rain (though this may technically be a misnomer)[89], the latent heating and cooling of which lead to temperature perturbations within the MCS. Mesoscale regions of high and low pressure subsequently develop: a mesohigh within the cold pool (owing to cold downdrafts that hydrostatically produce high pressure), and mesolows at mid-levels and behind the MCS (owing to warming resulting from latent-heat release)[90] (FIG. 5). The mid-level low pressure drives mesoscale convergence into the system, further supporting its maintenance, and is also key to the formation of the rear-inflow jet[62].

In comparison to internally driven MCSs, the externally driven counterparts have been relatively less studied. Nevertheless, modelling efforts and field campaigns reveal that they most commonly form on the cool side

a Translating cold front pattern

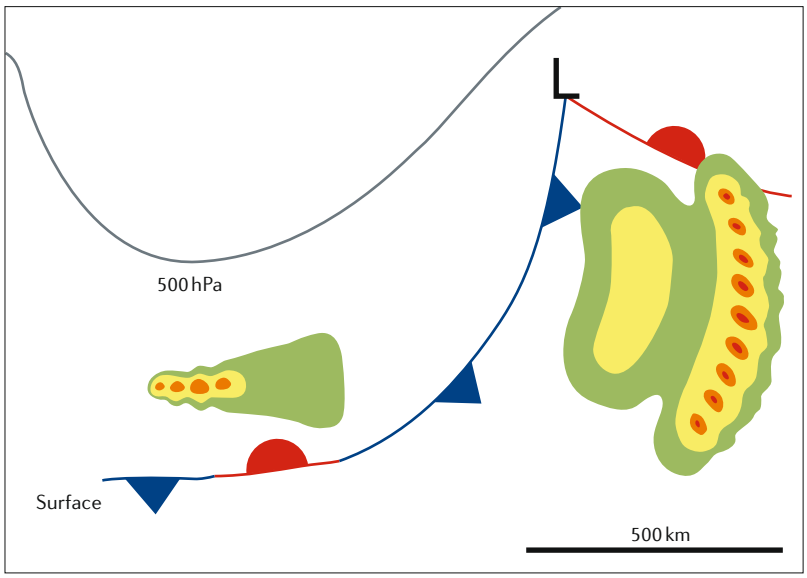

b Quasistationary east–west front pattern

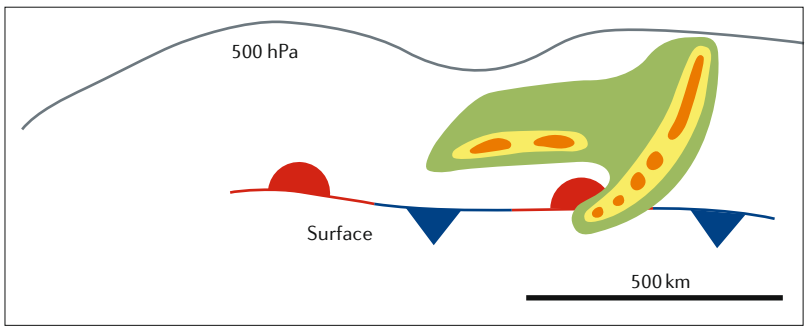

Fig. 4 | **Common environments for MCS formation and maintenance.** Synoptic environments conducive for mesoscale convective system (MCS) formation in a translating cold front (panel **a**) and quasistationary east–west front (panel **b**). Schematics illustrate common MCS types observed in those environments, consistent with the definitions shown in FIG. 1. Solid black lines indicate a 500-hPa geopotential height contour. Red lines with half-circles, blue lines with triangles, and alternating patterns represent warm, cold and stationary surface fronts, respectively. MCSs form in environments where the required ingredients of moisture, instability, lift and vertical wind shear are brought together; these two examples highlight two such common regimes in mid-latitudes. Adapted with permission from REF.[71], © American Meteorological Society.

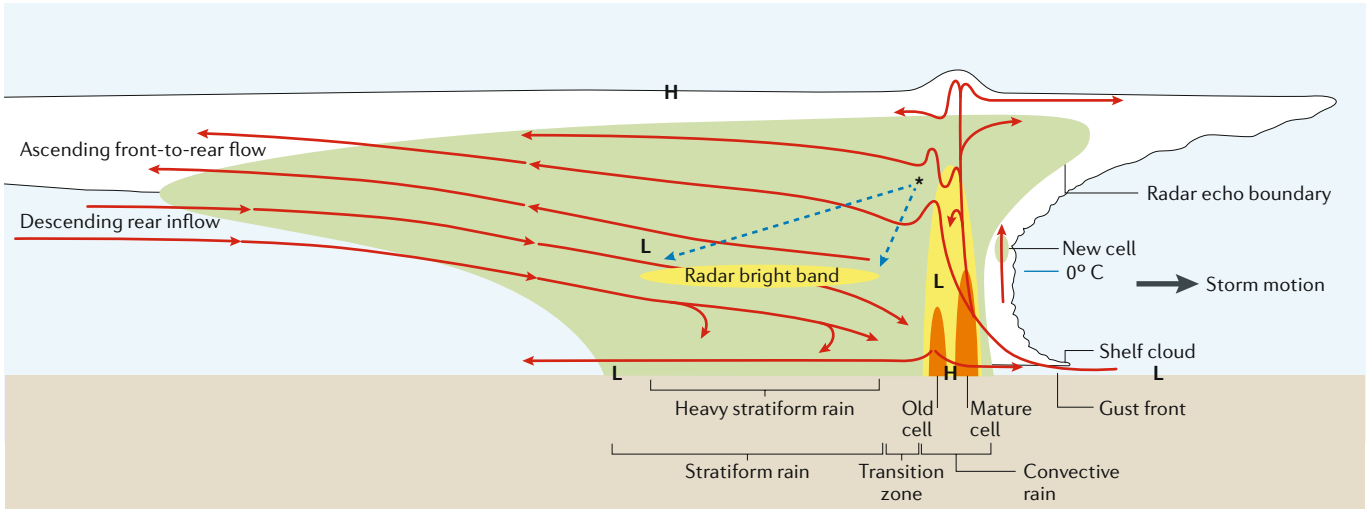

Fig. 5 | **Conceptual model of a squall line.** The vertical cross section is oriented perpendicular to the convective line, with a trailing stratiform region. The green shading indicates regions where radar echo is present (that is, where precipitation-sized hydrometeors are observed), with yellow and orange representing stronger radar echoes. Pressure minima and maxima are represented by 'L' and 'H', respectively. The height of the melting level is located just above that of the radar bright band, depicted by the black star and dashed blue arrows. Red arrows indicate the airflow within the mesoscale convective system, including ascending flow from front to rear and descent in a rear-inflow jet. Adapted with permission from REF.[90], © American Meteorological Society.

of a front or slow-moving boundary (FIG. 4b). In these scenarios, a low-level jet transports moist, unstable air that is lifted over a wedge-shaped region of cool air to the north of the boundary[67,76,78]. Convection then initiates, subsequently organizing into an MCS that is initially aligned parallel to the lifting boundary. Owing to the stable air near the surface on the cool side of the front, cold downdrafts experience resistance to sinking all the way to the surface[91]. In many cases, a cold pool does eventually form. However, in such environments wherein convection is initiated by large-scale ascent, cold-pool lifting is not required to maintain the convective system[92,93]. The interaction of convective downdrafts with near-surface stable layers (formed either from the pre-existing boundary or nocturnal cooling) generates many types of gravity waves; these waves generally are not fundamental to maintaining the MCS but they may organize the convection into linear structures and influence the distribution of precipitation[93–95].

Life cycle. Following formation and maintenance (through either cold-pool convection or frontal uplift), MCSs often transition between organizational modes during their life cycle[4,24]. One frequently observed example is the transition from a squall line (FIG. 1b) to a bow echo (FIG. 1c), a result of the formation of the rear-inflow jet as the cold pool strengthens[96–98]. Likewise, MCSs that initially are oriented parallel to the vertical wind shear will often reorient themselves to become perpendicular to the shear as cold-pool lifting is maximized[63,80].

MCSs can also transition to produce mesoscale convective vortices (MCVs), which are hundreds of kilometres across and, in some cases, persist for multiple days. The formation of an MCV can take place in two ways. One is from a bow echo: as the leading edge of the bow echo surges forward, a pair of counterrotating 'bookend vortices' form on the flanks of the surge. In some cases, the cyclonic vortex grows in spatial extent to be greater than 100 km in radius. An MCV can also emerge from the cumulative effects of latent heating in an MCS: where heating increases with height, a mesoscale region of low pressure forms (FIG. 5) and, as the Coriolis force acts on the convergent flow towards that low pressure, over time, a cyclonic circulation may develop. MCVs can prolong the lifetime of the MCS they originate from[99] and, in some instances, they initiate and maintain MCSs on subsequent days[100–103].

Eventually, MCSs must also dissipate, the processes of which have received relatively little attention. However, given that the frequency of MCS occurrence is often closely tied to the diurnal cycle, at least over land (FIG. 2), it follows that MCSs dissipate mainly because of processes that change with the diurnal cycle. Indeed, over continental regions that are prone to MCSs, low-level jets (which provide much of the moisture, instability and lift that support MCSs) weaken in the mid-morning hours, often leading to MCS dissipation[104]. Some squall lines also dissipate as their cold pools become strong enough to overwhelm the vertical shear, tilting the updrafts far rearwards[84].

Hazards and impacts from MCSs

Owing to the range of hazardous weather they produce, MCSs have been the subject of much scientific investigation, so as to improve forecasting and reduce societal risk and impact. Here, we outline the various hazards associated with MCSs, with a primary focus on damaging windstorms and flash flooding from heavy rains.

Severe winds and derechos. It has long been established that organized thunderstorms can produce widespread destruction, the majority of which is linked to persistent

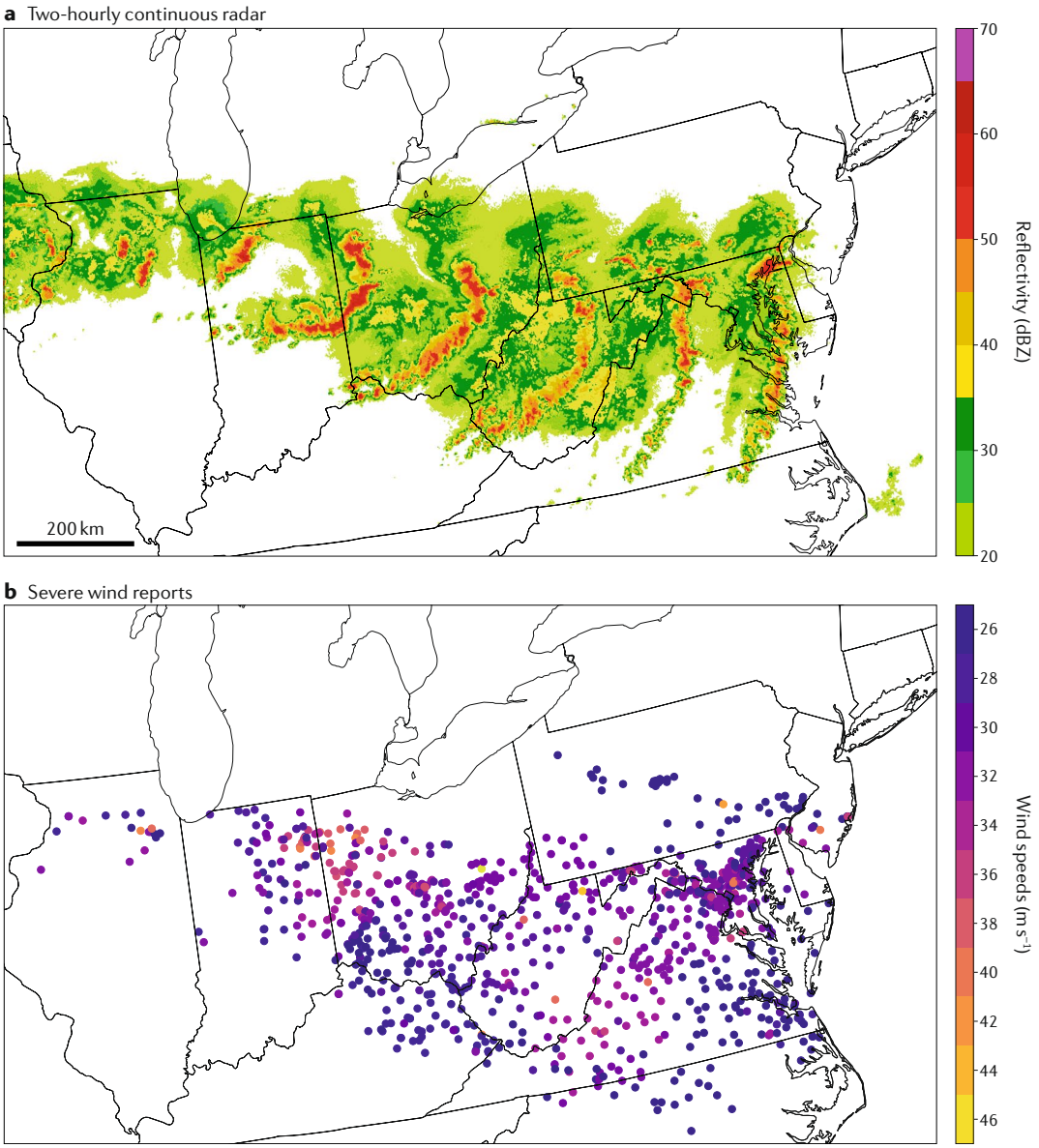

Fig. 6 | **Derecho impacts.** Two-hourly radar continuity map from 1600 UTC 29 June to 0400 UTC 30 June 2012 (panel **a**). Storm Prediction Center severe wind reports for the 29–30 June 2012 progressive derecho (panel **b**). Note that many of the wind speeds contained in the Storm Prediction Center data are estimated. Long-lived bow echoes are capable of producing broad swaths of damaging winds, known as derechos. This event resulted in 22 fatalities and millions of power outages. Radar data in panel **a** from GridRad[184]. Adapted with permission from REF.[106], © American Meteorological Society.

straight-line winds, or a derecho[105]. Derechos describe any family of downburst clusters associated with an MCS wherein winds of at least 58 mph (25.7 m s^{-1}) are observed in a swath at least 400 km long[9]. Damaging derechos have been exhibited in the USA[9,106], Europe[107], China[108] and South America[109]. On 29–30 June 2012, a particularly destructive example occurred from the midwestern to eastern USA (FIG. 6), with severe winds that exceeded 40 m s^{-1}, resulting in 22 fatalities, widespread damage and power outages affecting millions of people[13,106]. The environmental impact of derechos can also be staggering, as observed in the Amazon rainforest, where a squall line in January 2005 is estimated to have killed more than 500 million trees[109], and in North America in July 2009, where an estimated 25 million trees were blown down from northern Minnesota through to Ontario and Quebec[110].

Derechos have been classified according to two primary types of damage swath: progressive, where a single, fast-moving MCS produces the severe wind gusts, and serial, where a series of smaller swaths of damaging winds are observed within the broader swath[9]. Progressive derechos are often associated with a long-lived, fast-moving bow echo (FIG. 1c), specifically, the strong downdrafts in the cold pool and the descending rear-inflow jet[97,111] (FIG. 5). Smaller regions of strong rotation, known as mesovortices, can also form at the leading edge of the bow echo and locally intensify the winds and damage[112]. Serial derechos, on the other hand, are associated with MCSs forced by fronts and do

not necessarily depend on cold-pool or rear-inflow jet processes[113]; they typically produce a very large swath of strong winds, but not necessarily the extreme wind speeds often observed with progressive derechos. As a result, it has been proposed that the term 'derecho' be reserved for windstorms produced by bow echoes[111].

Heavy rainfall and flash floods. Although MCS-related rainfall is a key contributor to local and regional hydrological cycles, the abundance of extreme rainfall in many instances can also be hazardous. Slow-moving MCSs (or those organized in a way that allows the repeated passage of convective cells, termed echo training), for example, can produce substantial accumulations of precipitation over small geographic areas. Indeed, much like MCSs contribute a substantial fraction of total rainfall (FIG. 2), they are also responsible for a large proportion of extreme rain events throughout North America[10,114] and South America[36], as well as East Asia[115]. In the USA, for instance, 60–75% of extreme-rainfall events can be linked to the passage of MCSs[10] but only ~35% in eastern China[115]. Given such extreme rain potential, MCSs are closely related to flash flooding due to both extreme rainfall rates and prolonged duration. These floods can be deadly: as examples, an MCS over Beijing in July 2012 produced over 400 mm of rain and caused 79 fatalities[116], and a series of MCSs caused catastrophic flooding and 193 fatalities in Leh, India in August 2010 (REF.[12]).

Rainfall rates in MCSs have been shown to be a complex function of relative humidity, vertical wind shear and storm structure[117]. Specifically, high rain rates occur when the ingredients for moist convection are brought together such that moist air ascends rapidly (most commonly in deep convection), and that most of the condensate reaches the ground as rain (as opposed to evaporating or forming frozen precipitation)[117]. MCS rainfall, for example, is very sensitive to the amount of water vapour in the environment[118,119], and when synoptic and mesoscale conditions allow for the persistent transport of water vapour into a region favourable for MCSs, particularly extreme rainfall can take place. For instance, the transport of moisture ahead of a recurving tropical cyclone can greatly enhance the rainfall amounts in an already conducive environment[120–122]. Similarly, atmospheric rivers (narrow corridors of strong water vapour transport)[123] have been shown to contribute to some of the most extreme MCS-related rainfall events, such as the May 2010 flooding in Tennessee[124]. Both these situations can also promote the repeated development of MCSs over an extended time period, as observed in the Tennessee flooding example, further exacerbating flood potential.

MCSs can also be effective at yielding long-duration rainfall, particularly in TL-AS (FIG. 1d) and BB (FIG. 1e) organizations[5]. TL-AS MCSs are characterized by a line of convection on the cool side of, and approximately parallel to, a warm or stationary front[125] (as depicted in FIG. 4b, for example). In this scenario, the convective line (as well as an adjacent region of stratiform precipitation that develops farther towards the cool side of the boundary) moves from left to right with the upper-level winds, resulting in the repeated passage of heavy-rain-producing convective cells for many hours[5]. A TL-AS MCS produced 383 mm of rain in August 2007, breaking a record for 24 h rainfall in the state of Minnesota and causing destructive flash flooding[121]. In contrast to the repeated passage of the same convective cells for TL-AS MCSs, BB MCSs exhibit continuous generation of new convective lines or clusters in the opposite direction of movement, such that the MCS as a whole is nearly stationary. Specifically, if the motion of individual convective cells has equal magnitude and nearly opposite direction as the propagation (where new cells are initiating with respect to existing ones), it is a particularly favourable situation for heavy rainfall[126,127]. Several different processes can serve as the lifting mechanism for BB MCSs, including pre-existing boundaries such as fronts or outflow boundaries, convectively generated gravity waves, MCVs or remnant tropical cyclones[94,102,128]. Interestingly, at the same time as the aforementioned TL-AS MCS in August 2007 was producing heavy rainfall in Minnesota, a BB MCS near a remnant tropical cyclone was causing flash flooding hundreds of kilometres to the south in Oklahoma[121].

MCSs may also have embedded small-scale rotation, which can enhance vertical motions and, thus, rain rates. Supercells, for instance, can produce large amounts of condensate, owing to their very intense updrafts, in part, related to upwards pressure perturbation accelerations link to rotation[117,129]. As some MCSs have supercell-like rotation embedded within them (such as in moist environments with large, low-level vertical shear), enhanced updrafts and rain rates can similarly be observed[130], as also verified by numerical model simulations[131].

Other hazards. Although derechos and heavy rainfall constitute the most common hazards observed with MCSs, hazards more typically associated with supercell thunderstorms (specifically, hail and tornadoes) can also occur. From 1996 to 2007, for example, 21% of tornadoes in the USA were produced by QLCSs, a subset of MCSs[11], albeit with marked geographic variability; in the Ohio River Valley into the south-eastern USA, for instance, over 50% of tornado reports were linked to such systems[11]. However, QLCS-related tornadoes are generally weaker than those produced by supercells, accounting for only ~20% of significant tornadoes (higher than Enhanced Fujita scale 2) based on US data from 2000 to 2008 (REF.[132]). Mesovortices embedded within squall lines and bow echoes are the most common process by which MCSs spawn tornadoes[112].

Much like tornadoes, severe hail (which poses substantial risk to life and property) is most often associated with supercells. However, MCSs do produce hail, albeit with specific size limitations. In the USA, for example, severe hail[133] (>25.4 mm diameter) has been observed in relation to MCSs, whereas significant severe hail (>50.8 mm) is very infrequently produced[132,134]. Indeed, supercells are the dominant hail producers in the USA, producing more than twice as many hail reports per system compared with MCSs[134]. In subtropical South America, by contrast, only 7% of hailstorms fall in the discrete thunderstorm category, compared with 84.5% in the multicell-organized category representing MCSs[135].

Thus, the unique environments supporting MCSs globally lead to a variation in the resulting hazardous impacts of hail.

Finally, the global distribution of lightning also shows similarity with locations of frequent MCSs and, in turn, large area-mean rainfall[21,136,137]. For example, field observations have shown that MCSs with significant convective and stratiform precipitation produce large quantities of lightning, with negative cloud-to-ground flashes preferred in the convective region and positive flashes in the stratiform region[138]. Although MCSs are copious lightning producers, analyses of lightning fatalities show that unorganized convection is, by far, the biggest killer, likely because the large, organized storms of MCSs will cause people to take shelter, but isolated storms catch people unaware[139].

Prediction and forecasting

Considering the hazardous weather associated with MCSs and their importance to hydrological cycles, there is considerable societal need for accurate forecasts. However, despite improvements[140], the forecasting performance of warm-season convective precipitation (much of which comes from MCSs) remains inadequate[141,142]. At operational centres, skill for both rainfall[142] and severe weather[143] forecasts is at a minimum in the summer, when MCSs are responsible for a substantial proportion of those phenomena. For example, in advance of the June 2012 derecho (FIG. 6), most numerical weather-prediction models gave no indication that any precipitation would develop, let alone a significant severe-weather event[13].

The generally poor forecasting skill for MCSs can be linked, in part, to the comparatively small spatial scales on which convection takes place, and the very sharp gradients between heavy precipitation and no precipitation. Indeed, prior to the early 2000s, computing constraints meant that numerical weather-prediction models could not be run at high enough resolution to explicitly represent convective storms, instead relying on convective parameterizations to represent complex processes. Thus, key processes like cold pools and mesoscale circulations, integral for MCS formation and corresponding precipitation, were not explicitly represented.

However, computing capabilities — coupled with increased understanding of convective processes[144] — have since led to a new era for forecasting, wherein convection is explicitly represented. Such convection-allowing or convection-permitting models, with horizontal grid spacing of 1–4 km, have been used experimentally since the mid-2000s, and operationally since the late 2000s[145–149]. These forecasts can provide highly detailed representations of MCS development and evolution, and, in some cases, they predict the timing and location with remarkable specificity. For example, specific model configurations predicted derechos in May 2009 (REF.[150]) and June 2012 (REF.[13]) and an extreme-rain-producing MCS in April 2016 (REFS[130,151]) with great accuracy. Improvements to physical parameterizations and the assimilation of radar observations into convection-permitting models have also yielded improvements to MCS forecasts[152]. Nevertheless, convection-permitting model forecasts do not solve all the challenges associated with predicting MCSs and, in some instances, have been shown to perform poorly[153] and exhibit substantial biases[154]. However, ongoing research into convection-permitting ensemble prediction systems[155–157], as well as new statistical techniques and machine-learning methods[158–161], offer emerging opportunities for improved MCSs forecasting.

Changes with anthropogenic warming

Similar motivations for better forecasting and prediction of MCSs — their hydrological importance and hazardous impacts — also spur the need to better understand potential changes on longer timescales, particularly in the context of anthropogenic warming. Much like with weather forecasts, however, progress has been hampered by modelling limitations, largely, the challenges in faithfully simulating MCSs[162,163]. Nevertheless, with better availability of comprehensive data sets and continued advances in modelling, there has been headway with examining observed and projected changes in MCS characteristics, a summary of which can be found in TABLE 1.

Manual classification methods initially revealed no significant change in heavy rainfall from MCSs across the USA over the 20th century[164]. Yet, more recent analyses suggest positive trends in springtime MCS intensity and frequency in the central and eastern USA over the period 1979–2014 (REF.[17]) and in the warm season over the period 1997–2018 (REF.[165]). Specifically, observations and reanalysis data indicate that the average lifetime of MCSs has increased by 4% per decade, reaching 7% per decade for very-long-lasting MCSs (those exceeding the 95th percentile). Moreover, MCS-related total and extreme rainfall is further found to have increased, particularly for the 5–30 mm h^{-1} bins. These changes are attributed to warming and a corresponding strengthening of the Great Plains low-level jet, which, as discussed previously, provides key moisture supplies for MCS formation.

Outside of the USA, similar changes in MCS characteristics have also been observed, but a comprehensive picture is lacking, owing to limited data availability. For instance, satellite observations demonstrate that increases in tropical precipitation from 1998 to 2009 can largely be explained by changes in the frequency of organized deep convection[166], consistent with a corresponding enhancement also observed over Eurasia, although not specific to MCSs in this region[167]. Moreover, a threefold increase in the frequency of the most intense MCSs is apparent over the West African Sahel since 1982, linked to increased wind shear and changes in the Saharan Air Layer[168]. Thus, despite limited spatial representation, it appears that MCSs in some regions have increased in frequency and in rainfall intensity over the past several decades.

From a theoretical standpoint, MCS-related precipitation may intensify and become longer lasting in a future, warmer climate, owing to increased atmospheric moisture[169–172]. Thermodynamic theory — that is, Clausius–Clapeyron scaling — projects that precipitation intensity will increase by 7% K^{-1}. Coarse-resolution

Table 1 | **Summary of changes in MCS properties with warming**

Variable	Sign of change	Confidence[a]	Refs
MCS characteristics and hazards			
Rainfall (rate and volume)	Increase	High	16–18,119,165, 171,172,185
Severe winds	Uncertain[b]	–	177
Speed of motion	Increase	Low	16
Organization	Uncertain[b]	–	16,17,119,173
Size	Increase	Medium	16,17,119,185
Frequency	Increase	Low	16,165,173
MCS environments			
Atmospheric moisture	Increase	High	14,15,177–181
Atmospheric instability	Increase	High	14,15,177–181
Convective inhibition	Increase	Medium	14,181
Vertical wind shear	Uncertain[b]	–	15,176,178
Frequency of environments supportive of MCSs	Increase	Low	15,17,165, 178,181

MCS, mesoscale convective system. [a]Confidence refers to the convergence of evidence based on different data sources and lines of inquiry. Confidence is rated as high for results that have been consistently found across numerous studies with both theoretical and modelling support. [b]Uncertainty arises owing to inadequate investigation and, as such, there is no estimate of confidence. For MCS organization, there is confidence that changes will occur, but there is uncertainty in what those changes will be, including the sign.

models, however, predict scaling closer to 3–4% K^{-1}, although changes in convection-permitting regional models are closer to or exceed the expected Clausius–Clapeyron theory[16,18,172]. Therefore, simulating projected changes in MCS characteristics with high fidelity also requires high-resolution modelling to adequately resolve important microscale-to-mesoscale processes.

Indeed, simulations using a convection-permitting regional climate model in the USA have found that, under a high emissions scenario (RCP8.5), the frequency of summertime MCSs will more than triple in some locations by the end of the century, with a simultaneous increase in total precipitation volume by 80%[16]. By contrast, different analyses of the same model output suggest that all MCS archetypes (linear and non-linear, including QLCSs) decreased in frequency in the future[173]. However, these decreases were attributed to a summertime warm bias in surface temperature over the USA impacting both convection-permitting[16,174] and global-climate models[175]. Convection-permitting simulations over Africa also project increases of 28% in heavy rainfall from MCSs[176]. For other hazards, such as severe winds, future changes are less certain[177,178].

In addition to the aforementioned studies explicitly simulating MCS characteristics under warming, research has also been carried out to understand how the thermodynamic environments conducive to MCS development may also evolve. CAPE was previously discussed as an important indicator of the ingredients necessary for convection, which, in the future climate, is projected to increase[14,15,177–181], given that the primary factors in the CAPE magnitude are temperature and moisture. However, the energy inhibiting convection from forming (convective inhibition) will also increase over land regions[14,181], primarily due to reduced low-level relative humidity, higher lifting condensation levels and level of free convection, and, therefore, more negative buoyancy[181]. Collectively, these thermodynamic changes explain a decrease in weak-to-moderate convection but an increase in strong convection[14], consistent with some observational studies[165]. In other words, the environment supporting convection in a future climate will have more energy available for convection, but also more energy inhibiting convection; thus, only the elements that can overcome this barrier will be able to realize this potential energy (that is, the most intense convection).

Summary and future perspectives

MCSs have been the focus of sustained research over the past several decades and, therefore, many of their key processes are now well understood. For example, it is known that development requires sufficient moisture and instability, along with a lifting mechanism to initiate convection, as well as vertical wind shear to organize the storms into a larger system. As a result, MCSs are commonly observed across the global tropics, and in many subtropical and mid-latitude areas, where these key ingredients are routinely provided, especially in summer. Vertical wind shear has been found to be a primary factor in determining the organization of MCSs, with greater shear promoting the formation of more organized MCSs, such as lines and bow echoes. Moreover, there has been considerable societal interest in the hazardous weather associated with MCSs and, as such, progress has been made in regards to understanding which MCSs are prone to producing extreme rainfall, damaging winds and tornadoes. Despite the importance, prediction of MCSs remains a major challenge. Improvements in model resolution, however, have spurred progress, which has also fed back to quantifying projected changes in MCSs under anthropogenic warming. Specifically, it is now generally thought that the intensity and volume of MCS-related precipitation will increase, along with increases in MCS frequency in some regions, some changes of which have already been observed in the USA.

Yet, despite profound progress, numerous opportunities for future research exist, which, in some cases, are urgently needed. In many parts of the world, understanding of MCSs and their impacts remains limited, including South America, Africa and many tropical locations. Thus, there is a clear need for the collection of more and better observations of the environments supporting the development and maintenance of MCSs (particularly moisture and vertical wind profiles), MCS processes themselves (including the properties of updrafts, downdrafts and cold pools) and their hazards, all of which will likely also yield improvements in forecasting. Both routine observations (from remote sensing platforms, such as radars and satellites) and targeted field-campaign efforts are needed in this regard; the 2018 RELAMPAGO project in Argentina is one successful example. Additional campaigns in MCS-prone regions, such as Africa, could similarly yield new insights about MCSs.

Likewise, continued research and development is needed on numerical models so that they can better represent key aspects of MCSs, such as rainfall processes, cold pools, hazardous weather such as severe surface winds, cloud microphysics and influences on the larger-scale environment. Integrating new data sets into numerical models, and sophisticated methods for post-processing of model output, will also yield important results. These advances are likely to first manifest in the models used for basic understanding and weather forecasting, but can then translate as well to the models used to project future climate scenarios.

In that regard, substantial progress is needed in both understanding existing observations of MCSs in a climate context, as well as reliably projecting future changes. Recently emerging longer-term data sets offer potential to investigate these changes. However, it is not just the frequency of MCSs that must be understood. With the potentially hazardous precipitation, there is also the need to understand MCS-related precipitation changes. Yet, observations of vertical profiles of moisture are limited and must be expanded to better assess future changes. Model analyses could further provide insight into changes under warming, but, to date, most analyses with convection-permitting regional climate models have been based on a single high-emissions scenario; exploration across multiple scenarios is needed to improve the representation of variability and sensitivity in future projections.

Historically, the fields of mesoscale meteorology and climate dynamics have followed separate paths with little overlap, in part, because specific weather systems primarily represent noise in the context of climate. With continually increasing computing and data-analysis capabilities, there are opportunities for these two previously disparate fields to connect and collaborate in a new line of inquiry that has been termed mesoscale climate dynamics. MCSs are a ripe subject for such investigations, because they involve processes that are the domain of meteorologists, but have major influences on (and are influenced in significant ways by) the larger climate system. Current efforts in high-resolution climate modelling[16,174] are one important approach, but new and creative approaches to integrate understanding and prediction of MCSs across scales are also needed.

The integration of methods from climate science and mesoscale meteorology will also point to other cross-disciplinary research opportunities. As one example, vulnerability to urban flash flooding requires information about MCS rainfall, but must also be informed by expertise and data from hydrology, urban planning, social sciences, communication and so on[182]. With the trend towards increasing urbanization around the world, and the likelihood of more intense rainfall from MCSs in the future, the risk of urban flooding is almost certain to increase. Solutions to this challenge will require research that crosses traditional disciplinary boundaries and provides information that is usable by decision makers.

Published online: 02 June 2020

1. Maddox, R. A. Mesoscale convective complexes. *Bull. Am. Meteorol. Soc.* **61**, 1374–1387 (1980).
2. Weisman, M. L. & Davis, C. A. Mechanisms for the generation of mesoscale vortices within quasi-linear convective systems. *J. Atmos. Sci.* **55**, 2603–2622 (1998).
3. Fujita, T. T. Manual of downburst identification for project NIMROD [National Intensive Meteorological Research on Downburst] (Univ. Chicago, 1978).
4. Parker, M. D. & Johnson, R. H. Organizational modes of midlatitude mesoscale convective systems. *Mon. Weather Rev.* **128**, 3413–3436 (2000).
5. Schumacher, R. S. & Johnson, R. H. Organization and environmental properties of extreme-rain-producing mesoscale convective systems. *Mon. Weather Rev.* **133**, 961–976 (2005).
6. Nesbitt, S. W., Cifelli, R. & Rutledge, S. A. Storm morphology and rainfall characteristics of TRMM precipitation features. *Mon. Weather Rev.* **134**, 2702–2721 (2006).
7. Haberlie, A. M. & Ashley, W. S. A radar-based climatology of mesoscale convective systems in the United States. *J. Clim.* **32**, 1591–1606 (2019).
Comprehensively performs long-term analysis of MCS rainfall and characteristics in the USA.
8. Junker, N. W., Schneider, R. S. & Fauver, S. L. A study of heavy rainfall events during the Great Midwest Flood of 1993. *Weather Forecast.* **14**, 701–712 (1999).
9. Johns, R. H. & Hirt, W. D. Derechos: widespread convectively induced windstorms. *Weather Forecast.* **2**, 32–49 (1987).
10. Stevenson, S. N. & Schumacher, R. S. A 10-year survey of extreme rainfall events in the central and eastern United States using gridded multisensor precipitation analyses. *Mon. Weather Rev.* **142**, 3147–3162 (2014).
11. Ashley, W. S., Haberlie, A. M. & Strohm, J. A climatology of quasi-linear convective systems and their hazards in the United States. *Weather Forecast.* **34**, 1605–1631 (2019).
12. Rasmussen, K. L. & Houze, R. A. Jr A flash-flooding storm at the steep edge of high terrain: disaster in the Himalayas. *Bull. Am. Meteorol. Soc.* **93**, 1713–1724 (2012).
13. National Oceanic and Atmospheric Administration. The historic derecho of June 29, 2012 (NOAA, 2013).
14. Rasmussen, K. L., Prein, A. F., Rasmussen, R. M., Ikeda, K. & Liu, C. Changes in the convective population and thermodynamic environments in convection-permitting regional climate simulations over the United States. *Clim. Dyn.* https://doi.org/10.1007/s00382-017-4000-7 (2017).
15. Diffenbaugh, N. S., Scherer, M. & Trapp, R. J. Robust increases in severe thunderstorm environments in response to greenhouse forcing. *Proc. Natl Acad. Sci. USA* **110**, 16361–16366 (2013).
16. Prein, A. F. et al. Increased rainfall volume from future convective storms in the US. *Nat. Clim. Change* **7**, 880–884 (2017).
17. Feng, Z. et al. More frequent intense and long-lived storms dominate the springtime trend in central US rainfall. *Nat. Commun.* **7**, 13429 (2016).
18. Westra, S. et al. Future changes to the intensity and frequency of short-duration extreme rainfall. *Rev. Geophys.* **52**, 522–555 (2014).
19. Houze, R. A. Jr Mesoscale convective systems. *Rev. Geophys.* **42**, RG4003 (2004).
20. Houze, R. A. Jr 100 years of research on mesoscale convective systems. *Meteorol. Monogr.* **59**, 17.1–17.54 (2018).
A historical perspective on MCS research.
21. Zipser, E. J., Cecil, D. J., Liu, C., Nesbitt, S. W. & Yorty, D. P. Where are the most intense thunderstorms on Earth? *Bull. Am. Meteorol. Soc.* **87**, 1057–1071 (2006).
22. Wang, J. et al. The detection of mesoscale convective systems by the GPM Ku-band spaceborne radar. *J. Meteorol. Soc. Japan* **97**, 1059–1073 (2019).
23. Schiesser, H. H., Houze, R. A. Jr & Huntreiser, H. The mesoscale structure of severe precipitation systems in Switzerland. *Mon. Weather Rev.* **123**, 2070–2097 (1995).
24. Dalal, S., Lohar, D., Sarkar, S., Sadhukhan, I. & Debnath, G. C. Organizational modes of squall-type mesoscale convective systems during premonsoon season over eastern India. *Atmos. Res.* **106**, 120–138 (2012).
25. Meng, Z., Yan, D. & Zhang, Y. General features of squall lines in East China. *Mon. Weather Rev.* **141**, 1629–1647 (2013).
26. Kuo, Y.-H. & Chen, G. T.-J. The Taiwan area mesoscale experiment (TAMEX): An overview. *Bull. Am. Meteorol. Soc.* **71**, 488–503 (1990).
27. Lee, T.-Y. & Kim, Y.-H. Heavy precipitation systems over the Korean peninsula and their classification. *Asia-Pac. J. Atmospheric Sci.* **43**, 367–396 (2007).
28. Houze, R. A. Jr, Smull, B. F. & Dodge, P. Mesoscale organization of springtime rainstorms in Oklahoma. *Mon. Weather Rev.* **118**, 613–654 (1990).
29. Geerts, B. Mesoscale convective systems in the southeast United States during 1994–95: A survey. *Weather Forecast.* **13**, 860–869 (1998).
30. Haberlie, A. M. & Ashley, W. S. A method for identifying midlatitude mesoscale convective systems in radar mosaics. Part I: Segmentation and classification. *J. Appl. Meteorol. Climatol.* **57**, 1575–1598 (2018).
31. Haberlie, A. M. & Ashley, W. S. A method for identifying midlatitude mesoscale convective systems in radar mosaics. Part II: Tracking. *J. Appl. Meteorol. Climatol.* **57**, 1599–1621 (2018).
32. Feng, Z. et al. Spatiotemporal characteristics and large-scale environments of mesoscale convective systems east of the Rocky Mountains. *J. Clim.* **32**, 7303–7328 (2019).
33. Laing, A. G. & Fritsch, J. M. The global population of mesoscale convective complexes. *Q. J. R. Meteorol. Soc.* **123**, 389–405 (1997).
34. Liu, C., Zipser, E. J., Cecil, D. J., Nesbitt, S. W. & Sherwood, S. A cloud and precipitation feature database from nine years of TRMM observations. *J. Appl. Meteorol. Climatol.* **47**, 2712–2728 (2008).
35. Liu, C. & Zipser, E. J. The global distribution of largest, deepest, and most intense precipitation systems. *Geophys. Res. Lett.* **42**, 3591–3595 (2015).

36. Rasmussen, K. L., Chaplin, M. M., Zuluaga, M. D. & Houze, R. A. Contribution of extreme convective storms to rainfall in South America. *J. Hydrometeorol.* **17**, 353–367 (2016).
37. Durkee, J. D., Mote, T. L. & Shepherd, J. M. The contribution of mesoscale convective complexes to rainfall across subtropical South America. *J. Clim.* **22**, 4590–4605 (2009).
38. Mathon, V., Laurent, H. & Lebel, T. Mesoscale convective system rainfall in the Sahel. *J. Appl. Meteorol.* **41**, 1081–1092 (2002).
39. Laing, A. G. & Fritsch, J. M. Mesoscale convective complexes over the Indian monsoon region. *J. Clim.* **6**, 911–919 (1993).
40. Zuluaga, M. D. & Houze, R. A. Jr Extreme convection of the near-equatorial Americas, Africa, and adjoining oceans as seen by TRMM. *Mon. Weather Rev.* **143**, 298–316 (2015).
41. Garstang, M., Massie, H. L. Jr, Halverson, J., Greco, S. & Scala, J. Amazon coastal squall lines. Part I: Structure and kinematics. *Mon. Weather Rev.* **122**, 608–622 (1994).
42. Zuluaga, M. D. & Houze, R. A. Jr Evolution of the population of precipitating convective systems over the equatorial Indian Ocean in active phases of the Madden–Julian oscillation. *J. Atmos. Sci.* **70**, 2713–2725 (2013).
43. Fritsch, J. M., Kane, R. J. & Chelius, C. R. The contribution of mesoscale convective weather systems to the warm-season precipitation in the United States. *J. Climate Appl. Meteorol.* **25**, 1333–1345 (1986).
44. Houze, R. A. Jr, Rasmussen, K. L., Zuluaga, M. D. & Brodzik, S. R. The variable nature of convection in the tropics and subtropics: A legacy of 16 years of the Tropical Rainfall Measuring Mission satellite. *Rev. Geophys.* **53**, 994–1021 (2015).
45. Morel, C. & Senesi, S. A climatology of mesoscale convective systems over Europe using satellite infrared imagery. II: Characteristics of European mesoscale convective systems. *Q. J. R. Meteorol. Soc.* **128**, 1973–1995 (2002).
46. Ding, Y. H. in *East Asian Monsoon* (ed. Chang, C.-P.) 3–53 (World Scientific, 2004).
47. Rehbein, A., Ambrizzi, T. & Mechoso, C. R. Mesoscale convective systems over the Amazon basin. Part I: climatological aspects. *Int. J. Climatol.* **38**, 215–229 (2018).
48. Fritsch, J. M. & Forbes, G. S. in *Severe Convective Storms. Meteorological Monographs* (ed. Doswell, C. A.) 323–357 (American Meteorological Society, 2001).
49. Carbone, R. E., Tuttle, J. D., Ahijevych, D. A. & Trier, S. B. Inferences of predictability associated with warm season precipitation episodes. *J. Atmos. Sci.* **59**, 2033–2056 (2002).
50. Nesbitt, S. W. & Zipser, E. J. The diurnal cycle of rainfall and convective intensity according to three years of TRMM measurements. *J. Clim.* **16**, 1456–1475 (2003).
51. Rife, D. L., Pinto, J. O., Monaghan, A. J., Davis, C. A. & Hannan, J. R. Global distribution and characteristics of diurnally varying low-level jets. *J. Clim.* **23**, 5041–5064 (2010).
52. Tuttle, J. D. & Davis, C. A. Corridors of warm season precipitation in the central United States. *Mon. Weather Rev.* **134**, 2297–2317 (2006).
53. Markowski, P. & Richardson, Y. *Mesoscale Meteorology in Midlatitudes* (Wiley-Blackwell, 2010).
54. Cotton, W. R., Bryan, G. H. & van den Heever, S. C. *Storm and Cloud Dynamics* (Academic, 2010).
55. Trapp, R. J. *Mesoscale-Convective Processes in the Atmosphere* (Cambridge Univ. Press, 2013).
56. Houze, R. A. Jr *Cloud Dynamics* (Academic, 2014).
57. Johns, R. H. & Doswell, C. A. III. Severe local storms forecasting. *Weather Forecast.* **7**, 588–612 (1992).
58. Schultz, D. M., Schumacher, P. N. & Doswell, C. A. III. The intricacies of instabilities. *Mon. Weather Rev.* **128**, 4143–4148 (2000).
59. Rotunno, R., Klemp, J. B. & Weisman, M. L. A theory for strong, long-lived squall lines. *J. Atmos. Sci.* **45**, 463–485 (1988).
60. Lafore, J.-P. & Moncrieff, M. W. A numerical investigation of the organization and interaction of the convective and stratiform regions of tropical squall lines. *J. Atmos. Sci.* **46**, 521–544 (1989).
61. Fovell, R. G. & Ogura, Y. Numerical simulation of a midlatitude squall line in two dimensions. *J. Atmos. Sci.* **45**, 3846–3879 (1988).
62. Weisman, M. L. The role of convectively generated rear-inflow jets in the evolution of long-lived mesoconvective systems. *J. Atmos. Sci.* **49**, 1826–1847 (1992).
63. Parker, M. D. Simulated convective lines with parallel stratiform precipitation. Part II: Governing dynamics and associated sensitivities. *J. Atmos. Sci.* **64**, 289–313 (2007).
64. LeMone, M. A., Zipser, E. J. & Trier, S. B. The role of environmental shear and thermodynamic conditions in determining the structure and evolution of mesoscale convective systems during TOGA COARE. *J. Atmos. Sci.* **55**, 3493–3518 (1998).
Explores the role of vertical wind shear in tropical MCSs.
65. Johnson, R. H., Aves, S. L., Ciesielski, P. E. & Keenan, T. D. Organization of oceanic convection during the onset of the 1998 East Asian summer monsoon. *Mon. Weather Rev.* **133**, 131–148 (2005).
66. Jorgensen, D. P. & Weckwerth, T. M. in *Radar and Atmospheric Science: A Collection of Essays in Honor of David Atlas* (eds Wakimoto, R. M. & Srivastava, R.) 75–103 (American Meteorological Society, 2003).
67. Laing, A. G. & Fritsch, J. M. The large scale environments of the global populations of mesoscale convective complexes. *Mon. Weather Rev.* **128**, 2756–2776 (2000).
A synthesis of meteorological regimes supporting MCCs around the world.
68. Rasmussen, K. L. & Houze, R. A. Jr. Convective initiation near the Andes in subtropical South America. *Mon. Weather Rev.* **144**, 2351–2374 (2016).
69. Trier, S. B., Davis, C. A. & Ahijevych, D. A. Environmental controls on the simulated diurnal cycle of warm-season precipitation in the continental United States. *J. Atmos. Sci.* **67**, 1066–1093 (2010).
70. Zhang, Y., Zhang, F., Davis, C. A. & Sun, J. Diurnal evolution and structure of long-lived mesoscale convective vortices along the Mei-Yu front over the East China Plains. *J. Atmos. Sci.* **75**, 1005–1025 (2018).
71. Trier, S. B., Davis, C. A., Ahijevych, D. A. & Manning, K. W. Use of the parcel buoyancy minimum (B_{min}) to diagnose simulated thermodynamic destabilization. Part II: Composite analysis of mature MCS environments. *Mon. Weather Rev.* **142**, 967–990 (2014).
72. Maddox, R. A. Large scale meteorological conditions associated with midlatitude mesoscale convective complexes. *Mon. Weather Rev.* **111**, 1475–1493 (1983).
73. Corfidi, S. F. Cold pools and MCS propagation: forecasting the motion of downwind-developing MCSs. *Weather Forecast.* **18**, 997–1017 (2003).
74. Peters, J. M. & Schumacher, R. S. Objective categorization of heavy-rain-producing MCS synoptic types by rotated principal component analysis. *Mon. Weather Rev.* **142**, 1716–1737 (2014).
Examines the meteorological regimes for heavy-rain-producing MCSs using objective analysis methods.
75. Song, F. et al. Contrasting spring and summer large-scale environments associated with mesoscale convective systems over the US Great Plains. *J. Clim.* **32**, 6749–6767 (2019).
76. Trier, S. B. & Parsons, D. B. Evolution of environmental conditions preceding the development of a nocturnal mesoscale convective complex. *Mon. Weather Rev.* **121**, 1078–1098 (1993).
77. Augustine, J. A. & Caracena, F. Lower-tropospheric precursors to nocturnal MCS development over the central United States. *Weather Forecast.* **9**, 116–135 (1994).
78. Moore, J. T., Glass, F. H., Graves, C. E., Rochette, S. M. & Singer, M. J. The environment of warm-season elevated thunderstorms associated with heavy rainfall over the central United States. *Weather Forecast.* **18**, 861–878 (2003).
79. Coniglio, M. C., Hwang, J. Y. & Stensrud, D. J. Environmental factors in the upscale growth and longevity of MCSs derived from Rapid Update Cycle analyses. *Mon. Weather Rev.* **138**, 3514–3539; Corrigendum, 139, 2686–2688 (2010).
80. Tuttle, J. D. & Carbone, R. E. Coherent regeneration and the role of water vapor and shear in a long-lived convective episode. *Mon. Weather Rev.* **132**, 192–208 (2004).
81. Peters, J. M. & Schumacher, R. S. The simulated structure and evolution of a quasi-idealized warm-season convective system with a training convective line. *J. Atmos. Sci.* **72**, 1987–2010 (2015).
82. Guan, P., Chen, G., Zeng, W. & Liu, Q. Corridors of Mei-Yu-season rainfall over eastern China. *J. Clim.* **33**, 2603–2626 (2020).
83. Trier, S. B., Davis, C. A. & Carbone, R. E. Mechanisms governing the persistence and diurnal cycle of a heavy rainfall corridor. *J. Atmos. Sci.* **71**, 4102–4126 (2014).
84. Weisman, M. L. & Rotunno, R. "A theory for strong long-lived squall lines" revisited. *J. Atmos. Sci.* **61**, 361–382 (2004).
85. Bryan, G. H., Knievel, J. C. & Parker, M. D. A multimodel assessment of RKW theory's relevance to squall-line characteristics. *Mon. Weather Rev.* **134**, 2772–2792 (2006).
86. Parker, M. D. Relationship between system slope and updraft intensity in squall lines. *Mon. Weather Rev.* **138**, 3572–3578 (2010).
87. Stensrud, D. J., Coniglio, M. C., Davies-Jones, R. P. & Evans, J. S. Comments on "'A theory for strong long-lived squall lines' revisited". *J. Atmos. Sci.* **62**, 2989–2996 (2005).
88. Coniglio, M. C., Corfidi, S. F. & Kain, J. S. Views on applying RKW theory: an illustration using the 8 May 2009 Derecho-producing convective system. *Mon. Weather Rev.* **140**, 1023–1043 (2012).
89. Houze, R. A. Jr Stratiform precipitation in regions of convection: a meteorological paradox? *Bull. Am. Meteorol. Soc.* **78**, 2179–2196 (1997).
90. Houze, R. A. Jr, Rutledge, S. A., Biggerstaff, M. I. & Smull, B. F. Interpretation of Doppler weather radar displays of midlatitude mesoscale convective systems. *Bull. Am. Meteorol. Soc.* **70**, 608–619 (1989).
91. Haertel, P. T., Johnson, R. H. & Tulich, S. N. Some simple simulations of thunderstorm outflows. *J. Atmos. Sci.* **58**, 504–516 (2001).
92. Crook, N. A. & Moncrieff, M. W. The effect of large-scale convergence on the generation and maintenance of deep moist convection. *J. Atmos. Sci.* **45**, 3606–3624 (1988).
93. Trier, S. B., Marsham, J. H., Davis, C. A. & Ahijevych, D. A. Numerical simulations of the postsunrise reorganization of a nocturnal mesoscale convective system during 13 June IHOP_2002. *J. Atmos. Sci.* **68**, 2988–3011 (2011).
94. Schumacher, R. S. Mechanisms for quasi-stationary behavior in simulated heavy-rain-producing convective systems. *J. Atmos. Sci.* **66**, 1543–1568 (2009).
95. Marsham, J. H. et al. Multi-sensor observations of a wave beneath an impacting rear-inflow jet in an elevated mesoscale convective system. *Q. J. R. Meteorol. Soc.* **136**, 1788–1812 (2010).
96. Adams-Selin, R. D. & Johnson, R. H. Mesoscale surface pressure and temperature features associated with bow echoes. *Mon. Weather Rev.* **138**, 212–227 (2010).
97. Weisman, M. L. The genesis of severe, long–lived bow echoes. *J. Atmos. Sci.* **50**, 645–670 (1993).
98. Weisman, M. L. Bow echoes: A tribute to TT Fujita. *Bull. Am. Meteorol. Soc.* **82**, 97–116 (2001).
99. Yang, Q., Houze, R. A. Jr, Leung, L. R. & Feng, Z. Environments of long-lived mesoscale convective systems over the central united states in convection permitting climate simulations. *J. Geophys. Res. Atmos.* **122**, 13,288–13,307 (2017).
100. Fritsch, J. M., Murphy, J. D. & Kain, J. S. Warm-core vortex amplification over land. *J. Atmos. Sci.* **51**, 1780–1807 (1994).
Thorough investigation of MCV intensification and persistence over continents.
101. Trier, S. B. & Davis, C. A. Influence of balanced motions on heavy precipitation within a long-lived convectively generated vortex. *Mon. Weather Rev.* **130**, 877–899 (2002).
102. Schumacher, R. S. & Johnson, R. H. Quasi-stationary, extreme-rain-producing convective systems associated with midlevel cyclonic circulations. *Weather Forecast.* **24**, 555–574 (2009).
103. Bosart, L. F. & Sanders, F. The Johnstown flood of July 1977: A long-lived convective system. *J. Atmos. Sci.* **38**, 1616–1642 (1981).
104. Gale, J. J., Gallus, W. A. J. & Jungbluth, K. A. Toward improved prediction of mesoscale convective system dissipation. *Weather Forecast.* **17**, 856–872 (2002).
105. Hinrichs, G. Tornadoes and derechos. *Am. Meteorol. J.* **5**, 341–349 (1888).
106. Guastini, C. T. & Bosart, L. F. Analysis of a progressive derecho climatology and associated formation environments. *Mon. Weather Rev.* **144**, 1363–1382 (2016).
107. Taszarek, M. et al. Derecho evolving from a mesocyclone–a study of 11 August 2017 severe weather outbreak in Poland: event analysis and high-resolution simulation. *Mon. Weather Rev.* **147**, 2283–2306 (2019).

108. Xia, R., Wang, D., Sun, J., Wang, G. & Xia, G. An observational analysis of a derecho in South China. *Acta Meteorol. Sin.* **26**, 773–787 (2012).
109. Negrón-Juárez, R. I. et al. Widespread Amazon forest tree mortality from a single cross-basin squall line event. *Geophys. Res. Lett.* **37**, L16701 (2010).
110. Minnesota Department of Natural Resources. Boundary waters: the fire next time (DNR, 2019).
111. Corfidi, S. F., Coniglio, M. C., Cohen, A. E. & Mead, C. M. A proposed revision to the definition of "Derecho". *Bull. Am. Meteorol. Soc.* **97**, 935–949 (2016).
112. Schenkman, A. D. & Xue, M. Bow-echo mesovortices: A review. *Atmos. Res.* **170**, 1–13 (2016).
113. Coniglio, M. C., Stensrud, D. J. & Richman, M. B. An observational study of derecho-producing convective systems. *Weather Forecast.* **19**, 320–337 (2004).
114. Schumacher, R. S. & Johnson, R. H. Characteristics of United States extreme rain events during 1999–2003. *Weather Forecast.* **21**, 69–85 (2006).
115. Zhang, L., Min, J., Zhuang, X. & Schumacher, R. S. General features of extreme rainfall events produced by MCSs over East China during 2016–17. *Mon. Weather Rev.* **147**, 2693–2714 (2019).
116. Zhang, D.-L. et al. The Beijing extreme rainfall of 21 July 2012: "Right results" but for wrong reasons. *Geophys. Res. Lett.* **40**, 1426–1431 (2013).
117. Doswell, C. A. III, Brooks, H. E. & Maddox, R. A. Flash flood forecasting: An ingredients-based methodology. *Weather Forecast.* **11**, 560–581 (1996).
118. Alfaro, D. A. & Khairoutdinov, M. Thermodynamic constraints on the morphology of simulated midlatitude squall lines. *J. Atmos. Sci.* **72**, 3116–3137 (2015).
119. Schumacher, R. S. & Peters, J. M. Near-surface thermodynamic sensitivities in simulated extreme-rain-producing mesoscale convective systems. *Mon. Weather Rev.* **145**, 2177–2200 (2017).
120. Galarneau, T. J. Jr, Bosart, L. F. & Schumacher, R. S. Predecessor rain events ahead of tropical cyclones. *Mon. Weather Rev.* **138**, 3272–3297 (2010).
121. Schumacher, R. S., Galarneau, T. J. Jr & Bosart, L. F. Distant effects of a recurving tropical cyclone on rainfall in a midlatitude convective system: a high-impact predecessor rain event. *Mon. Weather Rev.* **139**, 650–667 (2011).
122. Moore, B. J., Bosart, L. F., Keyser, D. & Jurewicz, M. L. Synoptic-scale environments of predecessor rain events occurring east of the Rocky Mountains in association with Atlantic basin tropical cyclones. *Mon. Weather Rev.* **141**, 1022–1047 (2013).
123. Payne, A. E. et al. Responses and impacts of atmospheric rivers to climate change. *Nat. Rev. Earth Environ.* **1**, 143–157 (2020).
124. Moore, B. J., Neiman, P. J., Ralph, F. M. & Barthold, F. E. Physical processes associated with heavy flooding rainfall in Nashville, Tennessee, and vicinity during 1–2 May 2010: the role of an atmospheric river and mesoscale convective systems. *Mon. Weather Rev.* **140**, 358–378 (2012).
125. Maddox, R. A., Chappell, C. F. & Hoxit, L. R. Synoptic and meso-α scale aspects of flash flood events. *Bull. Am. Meteorol. Soc.* **60**, 115–123 (1979).
126. Chappell, C. F. in *Mesoscale Meteorology and Forecasting* (ed. Ray, P. S.) 289–310 (American Meteorological Society, 1986).
127. Corfidi, S. F., Merritt, J. H. & Fritsch, J. M. Predicting the movement of mesoscale convective complexes. *Weather Forecast.* **11**, 41–46 (1996).
128. Kato, T. Quasi-stationary band-shaped precipitation systems, named "Senjo-Kousuitai", causing localized heavy rainfall in Japan. *J. Meteorol. Soc. Japan* https://doi.org/10.2151/jmsj.2020-029 (2020).
129. Smith, J. A., Baeck, M. L., Zhang, Y. & Doswell, C. A. Extreme rainfall and flooding from supercell thunderstorms. *J. Hydrometeorol.* **2**, 469–489 (2001).
130. Nielsen, E. R. & Schumacher, R. S. Dynamical mechanisms supporting extreme rainfall accumulations in the Houston "Tax Day" 2016 flood. *Mon. Weather Rev.* **148**, 83–109 (2020).
131. Nielsen, E. R. & Schumacher, R. S. Dynamical insights into extreme short-term precipitation associated with supercells and mesovortices. *J. Atmos. Sci.* **75**, 2983–3009 (2018).
132. Grams, J. S. et al. A climatology and comparison of parameters for significant tornado events in the United States. *Weather Forecast.* **27**, 106–123 (2012).
133. Cecil, D. J. & Blankenship, C. B. Toward a global climatology of severe hailstorms as estimated by satellite passive microwave imagers. *J. Clim.* **25**, 687–703 (2012).
134. Duda, J. D. & Gallus, W. A. Spring and summer midwestern severe weather reports in supercells compared to other morphologies. *Weather Forecast.* **25**, 190–206 (2010).
135. Bruick, Z. S., Rasmussen, K. L. & Cecil, D. J. Subtropical South American hailstorm characteristics and environments. *Mon. Weather Rev.* **147**, 4289–4304.
136. Albrecht, R. I., Goodman, S. J., Buechler, D. E., Blakeslee, R. J. & Christian, H. J. Where are the lightning hotspots on Earth? *Bull. Am. Meteorol. Soc.* **97**, 2051–2068 (2016).
137. Petersen, W. A. & Rutledge, S. A. On the relationship between cloud-to-ground lightning and convective rainfall. *J. Geophys. Res. Atmos.* **103**, 14025–14040 (1998).
138. Rutledge, S. A., Williams, E. R. & Petersen, W. A. Lightning and electrical structure of mesoscale convective systems. *Atmos. Res.* **29**, 27–53 (1993).
139. Ashley, W. S. & Gilson, C. W. A reassessment of US lightning mortality. *Bull. Am. Meteorol. Soc.* **90**, 1501–1518 (2009).
140. Bauer, P., Thorpe, A. & Brunet, G. The quiet revolution of numerical weather prediction. *Nature* **525**, 47–55 (2015).
141. Fritsch, J. M. & Carbone, R. E. Improving quantitative precipitation forecasts in the warm season: A USWRP research and development strategy. *Bull. Am. Meteorol. Soc.* **85**, 955–965 (2004).
142. Sukovich, E. M., Ralph, F. M., Barthold, F. E., Reynolds, D. W. & Novak, D. R. Extreme quantitative precipitation forecast performance at the Weather Prediction Center from 2001 to 2011. *Weather Forecast.* **29**, 894–911 (2014).
143. Herman, G. R., Nielsen, E. R. & Schumacher, R. S. Probabilistic verification of Storm Prediction Center convective outlooks. *Weather Forecast.* **33**, 161–184 (2018).
144. Lilly, D. K. Numerical prediction of thunderstorms — Has its time come? *Q. J. R. Meteorol. Soc.* **116**, 779–798 (1990).
145. Roberts, N. M. & Lean, H. W. Scale-selective verification of rainfall accumulations from high-resolution forecasts of convective events. *Mon. Weather Rev.* **136**, 78–97 (2008).
146. Weisman, M. L., Davis, C., Wang, W., Manning, K. W. & Klemp, J. B. Experiences with 0–36-h explicit convective forecasts with the WRF-ARW model. *Weather Forecast.* **23**, 407–437 (2008).
147. Schwartz, C. S. et al. Next-day convection-allowing WRF model guidance: a second look at 2-km versus 4-km grid spacing. *Mon. Weather Rev.* **137**, 3351–3372 (2009).
148. Kain, J. S. et al. Some practical considerations regarding horizontal resolution in the first generation of operational convection-allowing NWP. *Weather Forecast.* **23**, 931–952 (2008).
149. Xue, M. et al. Prediction of convective storms at convection-resolving 1 km resolution over continental United States with radar data assimilation: An example case of 26 May 2008 and precipitation forecasts from spring 2009. *Adv. Meteorol.* **2013**, 259052 (2013).
150. Weisman, M. L., Evans, C. & Bosart, L. The 8 May 2009 superderecho: Analysis of a real-time explicit convective forecast. *Weather Forecast.* **28**, 863–892 (2013).
151. Schumacher, R. S. Heavy rainfall and flash flooding. *Oxf. Res. Encycl. Nat. Hazard Sci.* https://doi.org/10.1093/acrefore/9780199389407.013.132 (2017).
152. Pinto, J. O., Grim, J. A. & Steiner, M. Assessment of the high-resolution rapid refresh model's ability to predict mesoscale convective systems using object-based evaluation. *Weather Forecast.* **30**, 892–913 (2015).
153. Zhang, F., Odins, A. M. & Nielsen-Gammon, J. W. Mesoscale predictability of an extreme warm-season precipitation event. *Weather Forecast.* **21**, 149–166 (2006).
154. Herman, G. R. & Schumacher, R. S. Extreme precipitation in models: an evaluation. *Weather Forecast.* **31**, 1853–1879 (2016).
155. Iyer, E. R., Clark, A. J., Xue, M. & Kong, F. A comparison of 36–60-h precipitation forecasts from convection-allowing and convection-parameterizing ensembles. *Weather Forecast.* **31**, 647–661 (2016).
156. Schwartz, C. S., Romine, G. S., Sobash, R. A., Fossell, K. R. & Weisman, M. L. NCAR's experimental real-time convection-allowing ensemble prediction system. *Weather Forecast.* **30**, 1645–1654 (2015).
157. Lawson, J. R. et al. Advancing from convection-allowing NWP to warn-on-forecast: evidence of progress. *Weather Forecast.* **33**, 599–607 (2018).
158. Ahijevych, D., Pinto, J. O., Williams, J. K. & Steiner, M. Probabilistic forecasts of mesoscale convective system initiation using the random forest data mining technique. *Weather Forecast.* **31**, 581–599 (2016).
159. Lagerquist, R., McGovern, A. & Smith, T. Machine learning for real-time prediction of damaging straight-line convective wind. *Weather Forecast.* **32**, 2175–2193 (2017).
160. Herman, G. R. & Schumacher, R. S. Money doesn't grow on trees, but forecasts do: forecasting extreme precipitation with random forests. *Mon. Weather Rev.* **146**, 1571–1600 (2018).
161. Herman, G. R. & Schumacher, R. S. 'Dendrology' in numerical weather prediction: what random forests and logistic regression tell us about forecasting extreme precipitation. *Mon. Weather Rev.* **146**, 1785–1812 (2018).
162. Gutowski, W. J. Jr et al. The ongoing need for high-resolution regional climate models: Process understanding and stakeholder information. *Bull. Am. Meteorol. Soc.* https://doi.org/10.1175/BAMS-D-19-0113.1 (2020).
163. Kooperman, G. J., Pritchard, M. S. & Somerville, R. C. J. The response of US summer rainfall to quadrupled CO_2 climate change in conventional and superparameterized versions of the NCAR community atmosphere model. *J. Adv. Model. Earth Syst.* **6**, 859–882 (2014).
164. Kunkel, K. E. et al. Meteorological causes of the secular variations in observed extreme precipitation events for the conterminous United States. *J. Hydrometeorol.* **13**, 1131–1141 (2012).
165. Hu, H., Leung, L. R. & Feng, Z. Observed warm-season characteristics of MCS and non-MCS rainfall and their recent changes in the central United States. *Geophys. Res. Lett.* **47**, e2019GL086783 (2020).
166. Tan, J., Jakob, C., Rossow, W. B. & Tselioudis, G. Increases in tropical rainfall driven by changes in frequency of organized deep convection. *Nature* **519**, 451–454 (2015).
167. Ye, H., Fetzer, E. J., Wong, S. & Lambrigtsen, B. H. Rapid decadal convective precipitation increase over Eurasia during the last three decades of the 20th century. *Sci. Adv.* **3**, e1600944 (2017).
168. Taylor, C. M. et al. Frequency of extreme Sahelian storms tripled since 1982 in satellite observations. *Nature* **544**, 475–478 (2017).
169. Trenberth, K. E., Dai, A., Rasmussen, R. M. & Parsons, D. B. The changing character of precipitation. *Bull. Am. Meteorol. Soc.* **84**, 1205–1218 (2003).
170. Del Genio, A. D. & Kovari, W. Climatic properties of tropical precipitating convection under varying environmental conditions. *J. Clim.* **15**, 2597–2615 (2002).
171. O'Gorman, P. A. & Schneider, T. The physical basis for increases in precipitation extremes in simulations of 21st-century climate change. *Proc. Natl Acad. Sci. USA* **106**, 14773–14777 (2009).
172. Ban, N., Schmidli, J. & Schär, C. Heavy precipitation in a changing climate: does short-term summer precipitation increase faster? *Geophys. Res. Lett.* **42**, 1165–1172 (2015).
173. Haberlie, A. M. & Ashley, W. S. Climatological representation of mesoscale convective systems in a dynamically downscaled climate simulation. *Int. J. Climatol.* **39**, 1144–1153 (2019).
174. Liu, C. et al. Continental-scale convection-permitting modeling of the current and future climate of North America. *Clim. Dyn.* **49**, 71–95 (2017).
175. Morcrette, C. J. et al. Introduction to CAUSES: Description of weather and climate models and their near-surface temperature errors in 5 day hindcasts near the Southern Great Plains. *J. Geophys. Res. Atmos.* **123**, 2655–2683 (2018).
176. Fitzpatrick, R. G. J. et al. What drives the intensification of mesoscale convective systems over the West African Sahel under climate change? *J. Clim.* **33**, 3151–3172 (2020).
177. Brooks, H. E. Severe thunderstorms and climate change. *Atmos. Res.* **123**, 129–138 (2013).

178. Gensini, V. A. & Mote, T. L. Estimations of hazardous convective weather in the United States using dynamical downscaling. *J. Clim.* **27**, 6581–6589 (2014).
179. Seeley, J. T. & Romps, D. M. Why does tropical convective available potential energy (CAPE) increase with warming? *Geophys. Res. Lett.* **42**, 10,429–10,437 (2015).
180. Romps, D. M. Clausius–Clapeyron scaling of CAPE from analytical solutions to RCE. *J. Atmos. Sci.* **73**, 3719–3737 (2016).
181. Chen, J., Dai, A., Zhang, Y. & Rasmussen, K. L. Changes in convective available potential energy and convective inhibition under global warming. *J. Clim.* **33**, 2025–2050 (2020).
182. National Research Council. *When Weather Matters: Science and Services to Meet Critical Societal Needs* (National Academies Press, 2010).
183. Zhang, J. et al. Multi-Radar Multi-Sensor (MRMS) quantitative precipitation estimation: initial operating capabilities. *Bull. Am. Meteorol. Soc.* **97**, 621–638 (2016).
184. Bowman, K. P. & Homeyer, C. R. GridRad — three-dimensional gridded NEXRAD WSR-88D radar data. *Res. Data Archive Natl Center Atmos. Res. Comput. Inform. Syst. Lab.* https://doi.org/10.5065/D6NK3CR7 (2017).
185. Lackmann, G. M. The south-central US flood of May 2010: present and future. *J. Clim.* **26**, 4688–4709 (2013).

Acknowledgements
The authors thank D. Lindsey, S. Nesbitt and A. Haberlie for providing data and updated figures. R.S.S. is supported by National Science Foundation grants AGS1636663, AGS-637244 and AGS-1661862 and NOAA grants NA18OAR4590308 and NA18OAR4590378. K.L.R. is supported by National Science Foundation grants AGS-1661657, AGS-1641167 and AGS-1854399.

Competing interests
The authors declare no competing interests.

Peer reviewer information
Nature Reviews Earth & Environment thanks Kathleen Schiro, Zhe Feng and the other, anonymous, reviewer(s) for their contribution to the peer review of this work.

Publisher's note
Springer Nature remains neutral with regard to jurisdictional claims in published maps and institutional affiliations.